# Three-dimensional numerical simulation of TIG welding with external magnetic field

Y. Kobayashi[1] , H. Komen[1], S. Matsuda[2] and M. Tanaka[1]

[1] *Joining and Welding Research Institute, Osaka University, Osaka, Japan*
[2] *University of the Ryukyus, Okinawa, Japan*

**Abstract:** Numerical simulation was performed to clarify the mechanism by which deep penetration was obtained by applying an external magnetic field to a tungsten inert gas welding. As a result, the deflection of an arc plasma, which was considered to be the cause of the decrease in the heat input, also increased the Lorentz force on a molten metal by narrowing the current path. Moreover, it is also suggested that the application of an external magnetic field increases the downward Lorentz force in the ECMP method, and that the Lorentz force transports the high-temperature molten metal on the weld pool surface to the bottom of the weld pool, resulting deep penetration.

**Keywords:** TIG welding, simulation, ECMP method, Lorentz force, weld pool convection

## 1. Introduction

An arc welding is a welding method in which a base metal that is a material to be welded is heated and melted by high-temperature arc plasma maintained between electrodes. Arc welding processes are classified into various types according to the type of electrode and gas type used, and an arc welding process using tungsten as the electrode and inert gases such as argon or helium as the shielding gas is called TIG (Tungsten Inert Gas) welding. This welding process is used for welding various metals because of its high cleanliness of welded metal. On the other hand, one of disadvantages of this process is that a penetration depth is shallower than in other welding processes.

In order to obtain the deeper penetration in TIG welding, previous studies have been conducted [1-3]. One of these is the ECMP (Electromagnetically Controlled Weld pool) method, in which the weld pool convection is controlled by the Lorentz forces enhanced by applied external magnetic field to the TIG welding process [4]. The penetration depth was deepened by this method compared to conventional TIG welding by increasing the downward Lorentz force acting on the weld pool by the external magnetic field. By weld pool surface observation using tracer particles, Matsuda et al. [5] experimentally clarified that the flow field on a weld pool surface during TIG welding with the ECMP method is different from that in the conventional TIG welding. However, it is still unclear how the applied external magnetic field changes the Lorentz force acting on the weld pool and how the Lorentz force acts to increase penetration depth.

In this study, a numerical simulation considering the external magnetic field was conducted to clarify the effect of the external magnetic field on arc phenomena and the mechanism of increased penetration.

## 2. Computational model

The velocity and the pressure of gas flow treated as an electromagnetic thermal fluid are obtained by solving mass and momentum conservation equations using the SIMPLE (Semi-Implicit Method for Pressure Linked Equation) method. Within a computational domain, the temperature is obtained from the energy conservation equation, and the current density is obtained by the Ohm's law and current conservation equation. The magnetic flux density is obtained by the Gauss's law and the Ampere's law. Furthermore, by adding the measured external magnetic flux density, TIG welding with ECMP method is simulated.

Figure 1. shows the computational domain used in this study. The computational domain is a three-dimensional Cartesian coordinate system consisting of a space of 44.2 mm in the $x$ and $y$-axis and 21.5 mm in the $z$-axis. Figure 1. shows the $y$-$z$ cross section through the central axis of a tungsten electrode, and the $x$-$z$ cross section through the central axis is similar. In addition, to facilitate understanding of the computational domain, the dimensions of each area are drawn without unification. This computational domain is divided into 51 heterogeneous control volumes in the $x$ and $y$ directions and 45 in the $z$ direction by the finite volume method. The minimum mesh size is $2.0\times10^{-1}$ mm in the $x$ and $y$ directions and $2.5\times10^{-1}$ mm in the $z$ direction at the tip of the electrode.

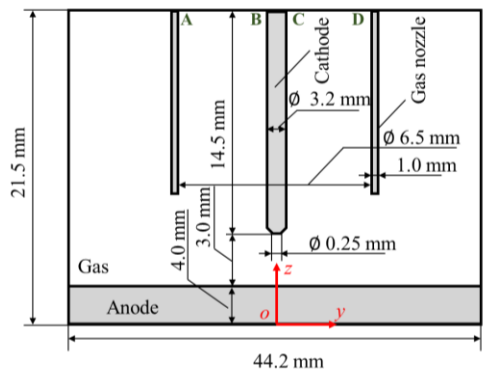


Fig. 1. Schematic illustration of computational domain for TIG arc model.

In this simulation, it is assumed that the plasma is in the local thermodynamic equilibrium, the gas flow is laminar, and the electrodes are not deformed by melting. Argon gas is supplied as the shielding gas from AB and CD in the gas nozzle in Fig. 1. at a total rate of 20 L/min. All other edges of the gas phase region are set as outlets.

A cathode was tungsten containing 2 wt.% lanthanum, an anode was water-cooled copper, and the welding current was set to 150 A.

## 3. Results and discussion

Figure 2. shows temperature distributions of conventional TIG welding and TIG welding with the ECMP method. The gray regions show the electrode and base metal, respectively. The high temperature region is deflected in the opposite direction of the welding direction due to the asymmetrical electromagnetic force caused by the external magnetic field. This arc deflection caused by the external magnetic field, which was observed in actual phenomena [6], is simulated.

Figure 3. shows the temperature distributions during TIG welding with the ECMP method obtained by imaging spectrometry and this simulation. From these results, it could be said that same tendencies of temperature distribution in experiment was obtained by simulation. The highest temperature obtained by experiment was 17,900 K, and the highest temperature obtained by simulation is 17,500 K. The *y*-axis width of the arc plasma at 11,000 K is 6.48 mm for the simulation and was 6.82 mm for the experiment. These results showed good agreement, although there was an error of about 5 %. These results showed the validity of this simulation.

Figure 4. shows the Lorentz force distributions in conventional TIG welding and TIG welding with the ECMP method. A white line shows the base metal surface, gray regions indicate electrode and gas nozzle. $L_y$ and $L_z$ are the Lorentz forces in the $y$ and $z$ directions. When the ECMP method is applied, the Lorentz force inside the base metal in the forward welding direction, indicated by point A′, increases compared to point A at the same location in conventional TIG welding. Incidentally, these coordinates A and A′ shown in this figure are $(x, y, z) = (0.0, 2.0, 3.8)$. The welding depth is considered to be affected by this difference in the Lorentz force distribution. Therefore, this difference in the Lorentz force distribution was investigated in detail.

$L_z$ is obtained by the following equation,

$$L_z = j_x B_y - j_y B_x. \qquad (1)$$

Here, $j_x$ and $j_y$ are current density in the $x$ and $y$ directions, and $B_x$ and $B_y$ are the magnetic flux density in the $x$ and $y$ directions, respectively. The values of $j_x$, $j_y$, $B_x$, $B_y$, $L_y$ and $L_z$ at A and A' are compared.

A

$$\begin{aligned}(j_x, j_y) &= (1.25 \times 10^5, -2.73 \times 10^6)\\ (B_x, B_y) &= (-6.45 \times 10^{-3}, 3.67 \times 10^{-5})\\ (L_y, L_z) &= (-2.60 \times 10^4, -1.55 \times 10^4)\\ (j_x B_y, j_y B_x) &= (4.59, 1.76 \times 10^4)\end{aligned}$$

A′

$$\begin{aligned}(j_x, j_y) &= (1.22 \times 10^5, -3.32 \times 10^6)\\ (B_x, B_y) &= (-9.49 \times 10^{-3}, 3.15 \times 10^{-5})\\ (L_y, L_z) &= (-3.50 \times 10^4, -2.80 \times 10^4)\\ (j_x B_y, j_y B_x) &= (3.84, 3.15 \times 10^4)\end{aligned}$$

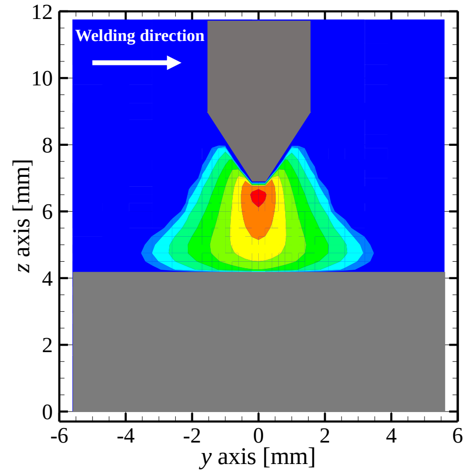


(a) Conventional TIG welding

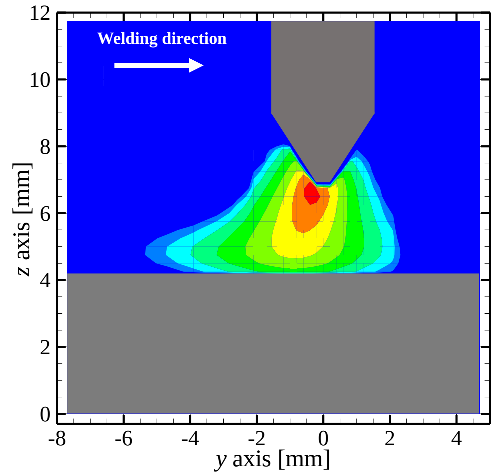


(b) TIG welding with ECMP method

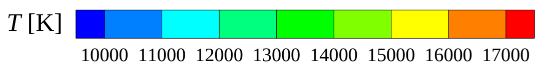


Fig. 2. Temperature distributions in (a) conventional TIG welding and (b) TIG welding the ECMP method.

At both points A and A′, $|j_y B_x|$ is much larger than $|j_x B_y|$. Therefore, it is shown that $j_y B_x$ is dominant in the Lorentz force in the $z$ direction. Comparing $j_y$, $B_x$ and $L_z$, A′ has a 21.6% increase in $|j_y|$, a 47.1% increase in $|B_x|$, and an 81.0% increase in $|L_z|$ compared to A. Especially, the increase in $|B_x|$ is caused by the external magnetic field applied in the $x$-axis direction. However, the increase in Lorentz force is caused not only by the increase in $|B_x|$, but also by the increase in $|j_y|$. This is because the current flows between tungsten electrode and base metal in the shortest path through the arc plasma deflected by the external magnetic field. Therefore, it is shown that in TIG welding with the ECMP method, the increase in $|B_x|$ due to the external magnetic field increases the downward Lorentz force the most, but the increase in $|j_y|$ due to arc deflection also increases the Lorentz force. Then, it is also suggested that the application of an external magnetic field increases the downward Lorentz force in the ECMP method, and that the Lorentz force transports the high-temperature molten metal on the weld pool surface to the bottom of the weld pool, resulting deep penetration.

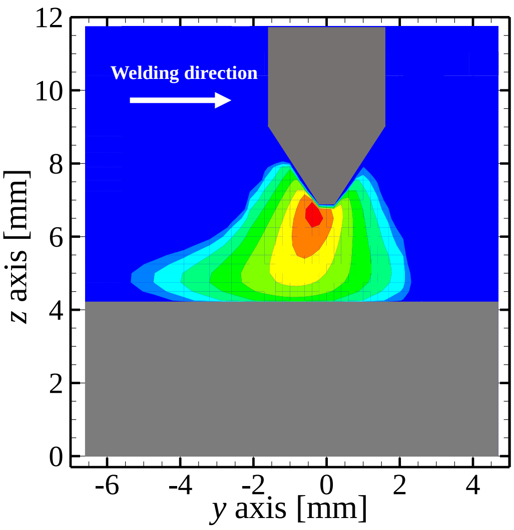


(a) Simulation

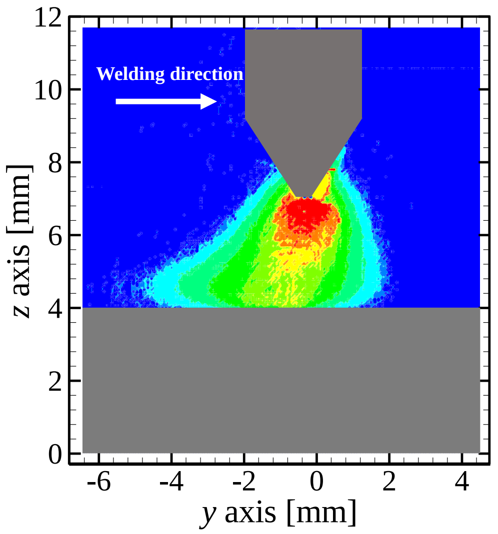


(b) Experiment

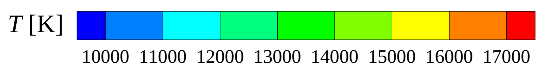


Fig. 3. Temperature distributions obtained by (a) simulation and (b) experiment.

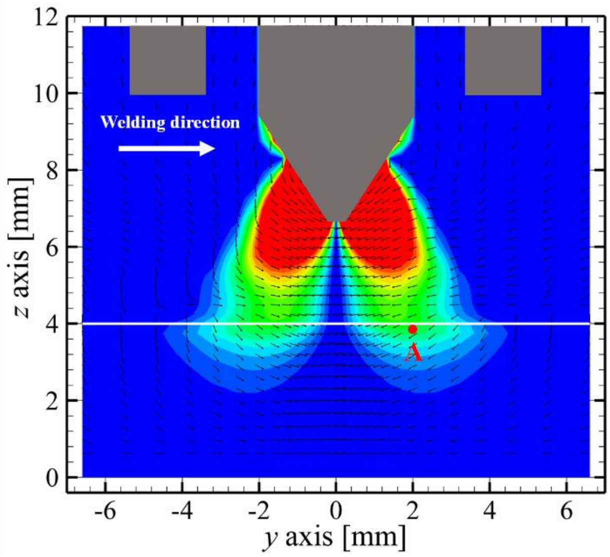


(a) Conventional TIG welding

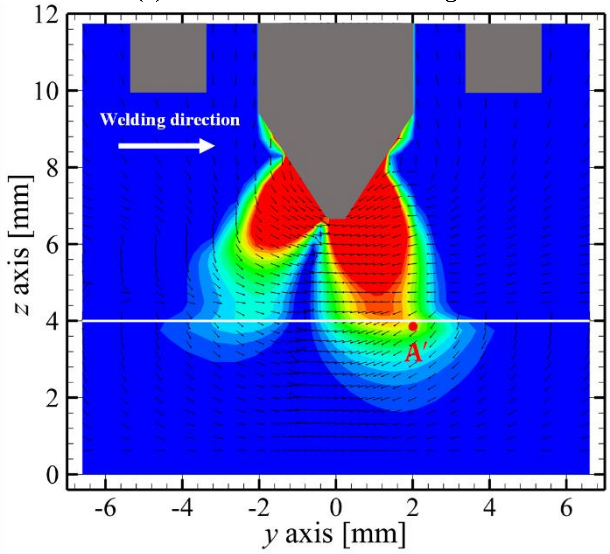


(b) TIG welding with ECMP method

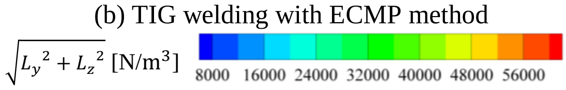


Fig. 4. Lorentz force distribution in (a) conventional TIG welding and (b) TIG welding with ECMP method.

## 4. References


[1] H. Fujii, Journal of Japan welding society, **74**, 3 (2005).

[2] M. Tanaka, Journal of Japan welding society, **74**, 2 (2005).

[3] M. Tanaka, Journal of Japan welding society, **71**, 2 (2002).

[4] S. Matsuda, Y. Manabe, K. Tamashiro, Y. Tanahara, Y. Matsumoto and Y. Matayoshi, Science and Technology of Welding and Joining, **30**, 2 (2012).

[5] T. Nakayama, S. Matsuda and Y. Tanahara, The Proceedings of Conference of kyushu, **72**, F22 (2019)

[6] L. Xiao, D. Fan and J. Huang, Journal of Manufacturing Processes, **32**, (2018)